Mesothelin-Specific Chimeric Antigen Receptor mRNA-Engineered T Cells Induce Antitumor Activity in Solid Malignancies

Gregory L. Beatty[1,3], Andrew R. Haas[1,2], Marcela V. Maus[1,3], Drew A. Torigian[1,5], Michael C. Soulen[1,5], Gabriela Plesa[1], Anne Chew[1], Yangbing Zhao[1,4], Bruce L. Levine[1,4,6], Steven M. Albelda[1,2], Michael Kalos[1,4], and Carl H. June[1,4,6]

Abstract

Off-target toxicity due to the expression of target antigens in normal tissue represents a major obstacle to the use of chimeric antigen receptor (CAR)-engineered T cells for treatment of solid malignancies. To circumvent this issue, we established a clinical platform for engineering T cells with transient CAR expression by using *in vitro* transcribed mRNA encoding a CAR that includes both the CD3-ζ and 4-1BB costimulatory domains. We present two case reports from ongoing trials indicating that adoptive transfer of mRNA CAR T cells that target mesothelin (CARTmeso cells) is feasible and safe without overt evidence of off-tumor on-target toxicity against normal tissues. CARTmeso cells persisted transiently within the peripheral blood after intravenous administration and migrated to primary and metastatic tumor sites. Clinical and laboratory evidence of antitumor activity was shown in both patients, and the CARTmeso cells elicited an antitumor immune response revealed by the development of novel antiself antibodies. These data show the potential of using mRNA-engineered T cells to evaluate, in a controlled manner, potential off-tumor on-target toxicities and show that short-lived CAR T cells can induce epitope spreading and mediate antitumor activity in patients with advanced cancer. Thus, these findings support the development of mRNA CAR-based strategies for carcinoma and other solid tumors. *Cancer Immunol Res; 2(2); 112–20. ©2013 AACR.*

Introduction

The adoptive transfer of genetically modified T cells engineered to express a chimeric antigen receptor (CAR) has produced early promising results for the treatment of patients with CD19^{+} hematologic malignancies (1–4). However, the application of CAR T cells to treat solid malignancies has been limited. This is due, at least in part, to the potential of CAR-based therapies to cause on-target off-tumor toxicity through their recognition of healthy cells that express the target antigen (5, 6). Several groups have evaluated safety approaches to circumvent the development

of potential adverse outcomes from the adoptive transfer of CAR T cells. Most often, these strategies have incorporated a safety, or "suicide," gene or more recently, an inducible caspase-9 transgene (7). However, the effectiveness of these strategies is potentially limited by their incomplete elimination of the transferred CAR T cells. As a result, there remains a need for an effective strategy to control the lifespan of adoptively transferred CAR T cells that can be evaluated for their safety in early clinical studies (8).

Mesothelin is a tumor-associated antigen that is overexpressed in the majority of malignant pleural mesotheliomas (MPM), pancreatic cancers, ovarian cancers, and some lung cancers (9, 10). Although mesothelin has a relatively limited expression pattern in normal tissues, it is expressed at low levels on normal peritoneal, pleural, and pericardial mesothelial surfaces. Mesothelin is a target of an endogenous immune response in MPM, ovarian cancer, and pancreatic cancer (11, 12). Clinical trials using antibody-based strategies to target mesothelin-expressing tumors have already shown initial safety and potential activity with serositis identified as a dose-limiting on-target off-tumor toxicity (13, 14). In preclinical studies, we observed potent antitumor effects with CAR T cells expressing an scFv-specific for mesothelin (15). Our approach to the clinic was to first evaluate mesothelin as a target using mRNA CAR cells.

We have shown the feasibility of using mRNA electroporation to engineer T cells with transient CAR expression (16–18).

Authors' Affiliations: [1]Abramson Cancer Center, Divisions of [2]Pulmonary and [3]Hematology-Oncology, Department of Medicine, Departments of [4]Pathology and Laboratory Medicine and [5]Radiology; and [6]Abramson Family Cancer Research Institute, Perelman School of Medicine, University of Pennsylvania, Philadelphia, Pennsylvania

Note: Supplementary data for this article are available at Cancer Immunology Research Online (http://cancerimmunolres.aacrjournals.org/).

G.L. Beatty, A.R. Haas, M. Kalos, and C.H. June contributed equally to this work.

Corresponding Authors: Carl H. June, University of Pennsylvania, 3400 Civic Center Boulevard, Room 123, Philadelphia, PA 19104-5156. Phone: 215-573-3269; Fax: 610-646-8455; E-mail: cjune@exchange.upenn.edu; and Gregory L. Beatty, Gregory.Beatty@uphs.upenn.edu

doi: 10.1158/2326-6066.CIR-13-0170

©2013 American Association for Cancer Research.

American Association for Cancer Research

This approach produced potent antitumor effects in preclinical xenograft models of human mesothelioma and advanced leukemia and established a cost-efficient and flexible platform for evaluating the safety and potential efficacy of novel CAR targets. Because of concerns for off-tumor toxicity with mesothelin-redirected T cells, we designed a clinical trial to evaluate the feasibility and safety of targeting mesothelin-positive tumors using T cells engineered to transiently express, by mRNA electroporation, a mesothelin-targeting CAR that incorporates the CD3ζ and 4-1BB signaling domains (CART-meso cells).

Here, we present two case reports from the first-in-human studies of mesothelin-specific mRNA CAR T cells in patients with mesothelin-expressing solid malignancies. We tested the feasibility of manufacturing mRNA-engineered T cells and the safety of repetitive infusion of CARTmeso cells in patients. Surprisingly, we observed clinical evidence for tumor responses and induction of a broad antitumor immune response consistent with epitope spreading in these two heavily pretreated patients with progressive disease. Our data thus support the feasibility of mRNA CAR T cells as a novel strategy for evaluating new therapeutic targets suitable for the treatment of patients with solid malignancies and suggest that mRNA CAR T cells may have therapeutic benefit.

Materials and Methods

Patients

Patient 17510-105 had advanced MPM and was enrolled into a phase I clinical trial (NCT01355965) at the Abramson Cancer Center, University of Pennsylvania (Philadelphia, PA). Inclusion criteria required age >18 years, Eastern Cooperative Oncology Group (ECOG) performance status (PS) of 0–1, adequate end-organ function, and histopathologic confirmation of either epithelial or biphasic MPM. Patients must have progressed on first-line therapy with a platinum pemetrexed-based doublet or decided not to pursue standard first-line chemotherapy. Patient 21211-101 had metastatic pancreatic cancer (PDA) and was included under a compassionate use study under the same approved Investigational New Drug (IND) application for NCT01355965. Exclusion criteria for both studies included active autoimmune disease requiring immunosuppressive therapy; prior gene therapy, or therapy with murine monoclonal antibodies; history of allergy to murine proteins; viral infection with HIV, HCV, or HBV; pregnancy; and any clinically significant pericardial effusion. Written informed consent was required. The study was approved by local institutional review boards. Both patients were elderly and had advanced chemotherapy-refractory cancer with extensive tumor burden at the time of enrollment (Supplementary Table S1).

Clinical protocols

Phase I clinical trial (NCT01355965) was designed to evaluate the manufacturing feasibility and safety of mRNA-transduced CARTmeso cells in patients with advanced MPM. Patient 17510-105 was given three infusions under schedule 1 and 2 of the protocol (Supplementary

Fig. S1B). PDA patient 21211-101 was given eight doses by i.v. infusion and two intratumoral injections under schedule 3 (Supplementary Fig. S1B). Detailed study design is described in the Supplementary Methods.

Cell lines

K562 (ATCC CCL-243) human erythroleukemia line, Panc-1 (ATCC CRL-1469) human pancreatic ductal adenocarcinoma, BxPc-3 (CRL-1687) human pancreatic ductal adenocarcinoma, and MiaPaCa (ATCC CRM-CRL-1420D) human pancreatic ductal adenocarcinoma were obtained from American Type Culture Collection (ATCC). All cell lines were banked at early passages and maintained in culture under the 6-month limit for recharacterization. Vials were thawed and maintained in culture for only several weeks at a time. REN, 208, 213, 302, 307, M30, and M60 were all derived from mesothelioma patient samples at the University of Pennsylvania. Cell line 21211 is a pancreatic adenocarcinoma line developed from ascites from a patient at the University of Pennsylvania. The K562 cells were obtained from ATCC, where the authenticated K562 cell line is deposited. Isoenzyme analysis was conducted and matched the isoenzymes listed on the ATCC website (http://www.atcc.org/Products/All/CCL-243.aspx#A7931A04156C4C7FA40828AEF707302F). The cell lines were free from mycoplasma contamination; except for transgene expression and isoenzyme analysis, no additional authentication was conducted.

CARTmeso cell manufacturing

The T cells were manufactured as specified by an U.S. Food and Drug Administration (FDA)-approved IND. Patients meeting eligibility criteria underwent a large-volume apheresis to isolate T cells for expansion and electroporation with an antimesothelin ss1 scFv CAR mRNA construct containing the 4-1BB and TCR-ζ signaling modules, as described previously (15). Clinical-grade in vitro–transcribed RNA was produced as described (16). For patient 21211 (PDA), autologous T cells were obtained from the patient's monozygotic twin brother. Briefly, T cells were activated by the addition of bead-immobilized anti-CD3 and anti-CD28 antibodies and cultured for 10 ± 2 days in cell culture medium supplemented with human serum. The expanded T cells were electroporated with mRNA encoding an antimesothelin ss1 scFv CAR using a closed system electroporation device (Maxcyte Inc.). The CARTmeso cells were then cryopreserved in an infusible cryoprotectant-supplemented solution. The infused cells were an average of 99.6% and 99.5% CD3$^+$ cells for the patient with MPM and PDA, respectively. For the patient with MPM and PDA respectively, 98.0% and 99.5% of the infused cells expressed the scFv as assessed by flow cytometry after electroporation. The cell viability was 91.4% (mean), with a range of 87.8% to 97.1% for the patient with MPM and 91.2% (mean) with a range of 76.0% to 98.6% for the patient with PDA. At the time of cell infusion, frozen CARTmeso cell aliquots were thawed and administered to patients in the Clinical Trials Research Center at the Hospital of the University of Pennsylvania. Supplementary Fig. S1A presents a summary of the manufacturing process for the RNA-modified T cells.

Sample collection and processing

Samples (peripheral blood, bone marrow) were collected in lavender top (K$_2$EDTA) or red top (no additive) Vacutainer tubes (Becton Dickinson). Research tubes were delivered to the laboratory within 2 hours of blood draw, and samples were generally processed within 30 minutes of receipt according to established laboratory standard operating procedures (SOP). Peripheral blood mononuclear cells were purified, processed, and stored in liquid nitrogen as described previously (19). Serum was isolated from red top tubes by centrifugation, aliquoted in single-use 100 to 200 µL aliquots, and stored at −80°C.

Ascites fluid analysis

On days +3 and +15 after beginning CARTmeso therapy, ascites was collected by large volume paracentesis on PDA patient 21211-101 as part of the standard of care. An automated total white blood cell count (cells/µL) of unprocessed ascites was determined and excess fluid was used to isolate cells by Ficoll-Paque processing, which were then cryopreserved. For multiparametric immunophenotyping, cryopreserved cells were thawed and stained at a density of 1×10^6 cells/100 µL PBS for 30 minutes on ice using antibody and reagent concentrations recommended by the manufacturer, washed, resuspended in 0.5% paraformaldehyde, and analyzed using a BD Fortessa (BD Immunocytometry) systems equipped with violet (405 nm), blue (488 nm), green (532 nm), and red (633 nm) lasers and appropriate filter sets for detection and separation of the following fluorescently conjugated antibodies: c-met, mesothelin, EpCAM, and CD45. Tumor cells were identified as mesothelin$^+$c-met$^+$. Tumor cell count within the ascites fluid was determined by multiplying the percentage of mesothelin$^+$c-met$^+$ cells by the total cell count/µL.

Real-time quantitative PCR analysis of RNA transcripts

Total RNA was isolated directly from whole blood, ascites, and tumor tissue using Ribopure blood kits (Ambion). cDNA synthesis was conducted using iScript cDNA synthesis kits (Biorad). cDNA was used in quantitative PCR (qPCR) assays to detect and quantify the abundance of transgene and CD3ε transcripts, using 1 µL cDNA reaction/amplification. The primer/probe set to detect transgene nucleic acid recognizes the 4-1BB-TCRζ junctional fragment in the signaling domain of the CAR molecule and has been described previously. To detect CD3ε transcripts, a TaqMan assay (Life Technologies) was used. To quantify levels of T cells and transgene in samples, a 9-point standard curve was generated using cDNA synthesized from RNA isolated from each final manufactured product, with a dilution range of 10% to 0.002%. Each data point (sample, standard curve) was evaluated in triplicate with a positive cycle threshold (C_t) value in three of three replicates with percentage coefficient of variance (CV) less than 20% for all quantifiable values. A parallel amplification reaction to control for the quality and quantity of interrogated cDNA was conducted using a primer/probe combination specific for the housekeeping gene *PP1B* and an ABI TaqMan assay (Life Technologies). These amplification reactions generated a normalization factor (NF) to normalize for input cDNA across samples. The

frequency of marked sample/CD3$^+$ T cell in each sample was calculated according to the formula: frequency of marked cells/total CD3$^+$ T cells = normalized transgene value/normalized CD3 value.

Analysis of serum soluble factors

Whole blood was collected in red top (no additive) Vacutainer tubes (Becton Dickinson), processed to obtain serum using established laboratory SOP, aliquoted for single use, and stored at −80°C. Quantification of soluble cytokine factors was conducted using Luminex bead array technology and kits purchased from Life technologies. Assays were conducted as per the manufacturer protocol with a 9-point standard curve generated using a 3-fold dilution series. The two external standard points were evaluated in duplicate and the five internal standards in singlet; all samples were evaluated in duplicate at 1:2 dilution; calculated %CV for the duplicate measures were less than 15%. Data were acquired on a FlexMAP-3D (Life Technologies) by percent and analyzed using XPonent 4.0 software (Life Technologies) and 5-parameter logistic regression analysis. Standard curve quantification ranges were determined by the 80% to 120% (observed/expected value) range. Reported values included those within the standard curve range and those calculated by the logistic regression analysis.

Detailed study design, cytotoxic T lymphocyte (CTL) assay, human anti-chimeric antibody (HACA) detection, Protoarray analysis, immunoblot analysis, and PET data acquisition and analysis are in Supplementary Methods.

Results

We report results from two cases showing the safety, feasibility, and antitumor effects of RNA CAR T-cell infusions in patients with refractory advanced cancer. Details of the study design are described in Supplementary Material. Patient 17510-105 had advanced MPM and was given three infusions under schedule 1 and 2 of the protocol (Supplementary Fig. S1B). Patient 21211-101 had metastatic pancreatic cancer (PDA) and was given eight doses by i.v. infusion and two intratumoral injections under schedule 3 (Supplementary Fig. S1B).

Safety of RNA CARTmeso cell infusions

Treatment-related adverse events are summarized in Supplementary Table S2. The safety and tolerability of the infusions are described in Supplementary Materials.

Humoral immune responses directed against CARTmeso cells

Immunoglobulin (IgG) HACA or human anti-mouse antibody (HAMA) responses were detected in both patients after CARTmeso infusions. Details are in Supplementary Materials.

Antitumor clinical activity of RNA CARTmeso cells

Both cases were evaluated for tumor response by computed tomographic (CT) imaging. In addition, patient 21211-101 was evaluated by [^{18}F]2-fluoro-2-deoxy-D-glucose (FDG) avidity on positron emission tomography/computed tomography (PET/CT) imaging before and after infusions (Fig. 1). Patient 17510-105 had stable disease after receiving CARTmeso T-cell
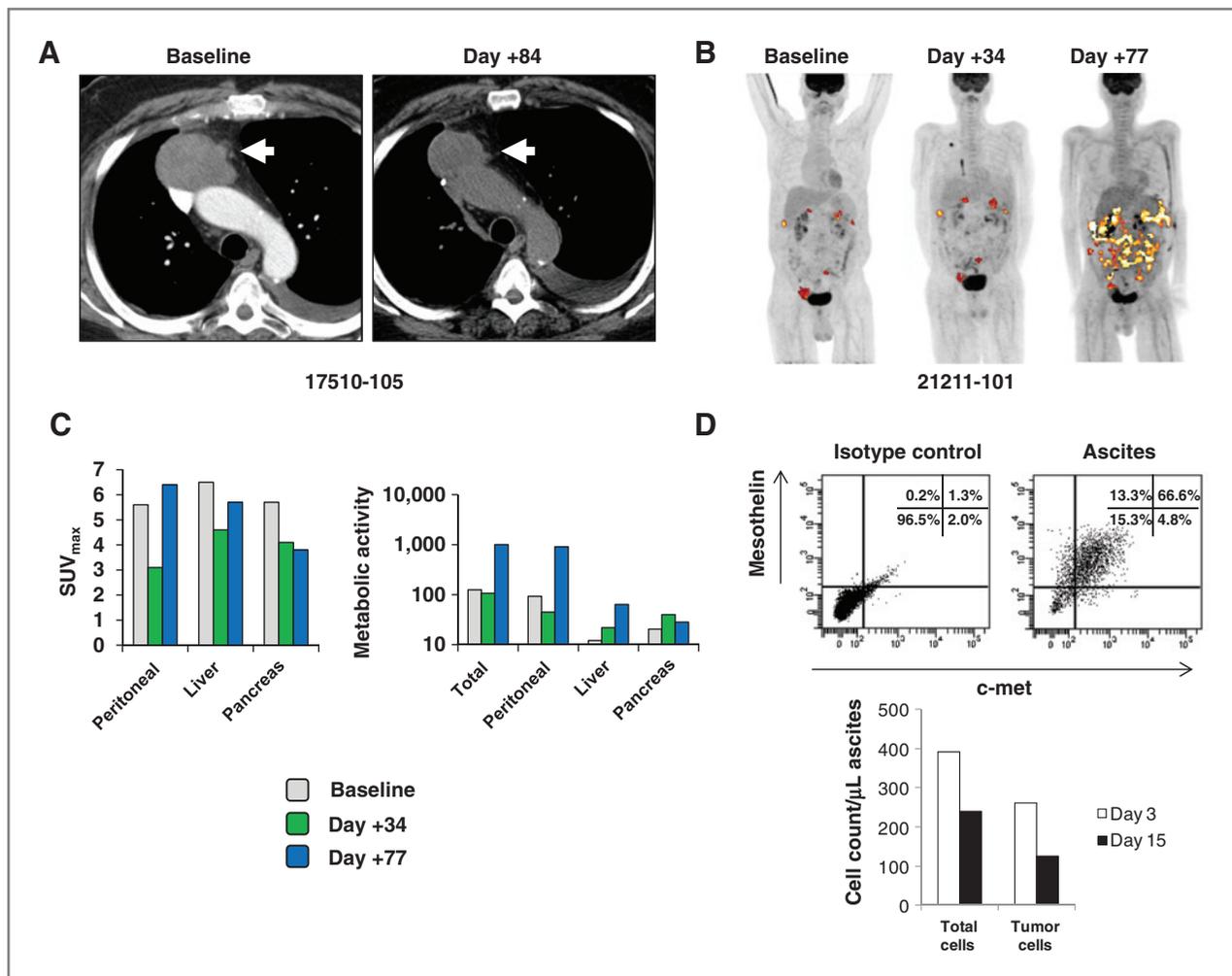
Figure 1. Antitumor activity of CARTmeso cells. A, CT imaging of MPM patient 17510-105 showing the patient's dominant mesothelioma mass before receiving CARTmeso infusion on schedule 1 (baseline) and 35 days after receiving the first CARTmeso infusion on schedule 2 (day +84). B, whole-body FDG PET/CT imaging of PDA patient 21211-101 obtained at baseline, day +34 after completing i.v. CARTmeso cell infusions, and day +77 after completing intratumoral CARTmeso cell infusions. C, analysis of maximum standardized uptake value (SUVmax) and mean metabolic volumetric product (MVPmean) at baseline, day +34, and day +77 is shown for all lesions (total) and individual sites of disease (peritoneal, liver, and pancreas) for PDA patient 21211-101. D, representative flow cytometric plot of ascites from PDA patient 21211-101 analyzed with isotype control antibodies versus antimesothelin and anti-c-met antibodies to identify mesothelin$^+$ c-met$^+$ tumor cells. Flow cytometric findings were quantified to determine the total number of cells/mL and tumor cells/μL in the ascites that is shown in the bar graph with comparison between day +3 and day +15 after beginning i.v. CARTmeso cell infusions.

infusions on schedule 1. However, this patient developed a confirmed partial response by the modified Response Evaluation Criteria in Solid Tumors (RECIST) after receiving one infusion of CARTmeso cells on schedule 2 (Fig. 1A). Disease progression was observed 6 months later. PDA patient 21211-101 had stable disease by RECIST 1.1 after completing 3 weeks of i.v. CARTmeso cell therapy. By FDG PET/CT imaging, a decrease in the maximum standardized uptake value (SUV$_{max}$) was seen in all sites of disease. To further quantify this metabolic response, changes in the mean volumetric product (MVP$_{mean}$) for each disease site were determined (Fig. 1B and C). A decrease in MVP$_{mean}$ was observed only in the peritoneal lesions. This effect was transient and was not sustained on repeat imaging obtained on day +77 after the completion of i.v.

injections on day +18. To understand the impact of CARTmeso cell therapy on peritoneal tumor burden, ascites fluid was analyzed by flow cytometry at defined time points after beginning therapy. Analysis of ascitic fluid on days +3 and +15 after beginning therapy revealed a 40% decrease in the concentration of tumor cells that coexpressed mesothelin and c-met (Fig. 1D). Overall, these findings suggest a role for CARTmeso cell infusions in inducing an antitumor effect in these two patients.

We also evaluated the impact of CARTmeso cell therapy using serologic tumor markers for both patients. Serum mesothelin-related peptide (SMRP) and CA19-9 levels were measured pre- and post-CARTmeso cell infusion. For patient 17510-105, SMRP levels initially increase during schedule 1 but then declined from

17 to 12 nmol/L after the patient received the first infusion of CARTmeso cells on schedule 2, consistent with a reduction in tumor burden seen by CT imaging. For PDA patient 21211-101, CA19-9 levels increased slowly over the course of treatment from 449 units/mL at baseline to 1,429 units/mL after completing i.v. CARTmeso cell therapy but remained stable thereafter for 1 month. However, after completion of the intratumoral injections of CARTmeso cells, the CA19-9 level began to increase again to 1,865 units/mL on day +59 and 2,271 units/mL by day +71, consistent with disease progression.

In vivo persistence and trafficking of RNA CARTmeso cells

A qPCR assay was developed to detect and quantify the persistence of CARTmeso cells in patients following infusion. Because the CARTmeso transgene is introduced and maintained in T cells as mRNA, reverse transcription was necessary before qPCR. Analysis of peripheral blood, ascites, and tumor samples from the patients are presented in Fig. 2. Within the peripheral blood, CARTmeso transgene was detected in both patients immediately following each infusion. Moreover, the levels of detected transgene at each time point during schedule 1 correlated with the infusion dose. In both cases, maximal levels were detected in the postinfusion time point collected within 2 hours of the infusion. In agreement with the biodegradable nature of the CARTmeso transgene, the levels decreased progressively on successive days. For the PDA patient 21211-101, additional infusions beyond 1 week produced lower levels of detectable CARTmeso transgene within the peripheral blood compared with the initial infusion (Fig. 2B).

Trafficking of CARTmeso cells to tumor tissues was evaluated in patient 21211-101 by collecting ascites at serial time points and by obtaining a tumor biopsy on day +35 of schedule 3. In each sample, CARTmeso transgene was detected, showing that mRNA CARTmeso cells are capable of trafficking to the extravascular tumor compartments (Fig. 2C). Within the ascites, CARTmeso transgene was detected 3 days after initial infusion and in subsequent samples obtained 6 days after the eighth infusion and 13 days after the first intratumoral injection of CARTmeso cells. Within the primary pancreatic tumor, high levels of CARTmeso transcripts were detected before the first intratumoral injection, whereas lower but significant levels were detected 22 days later on subsequent tumor biopsy. These findings show that CARTmeso cells can infiltrate solid tumors when delivered intravenously.
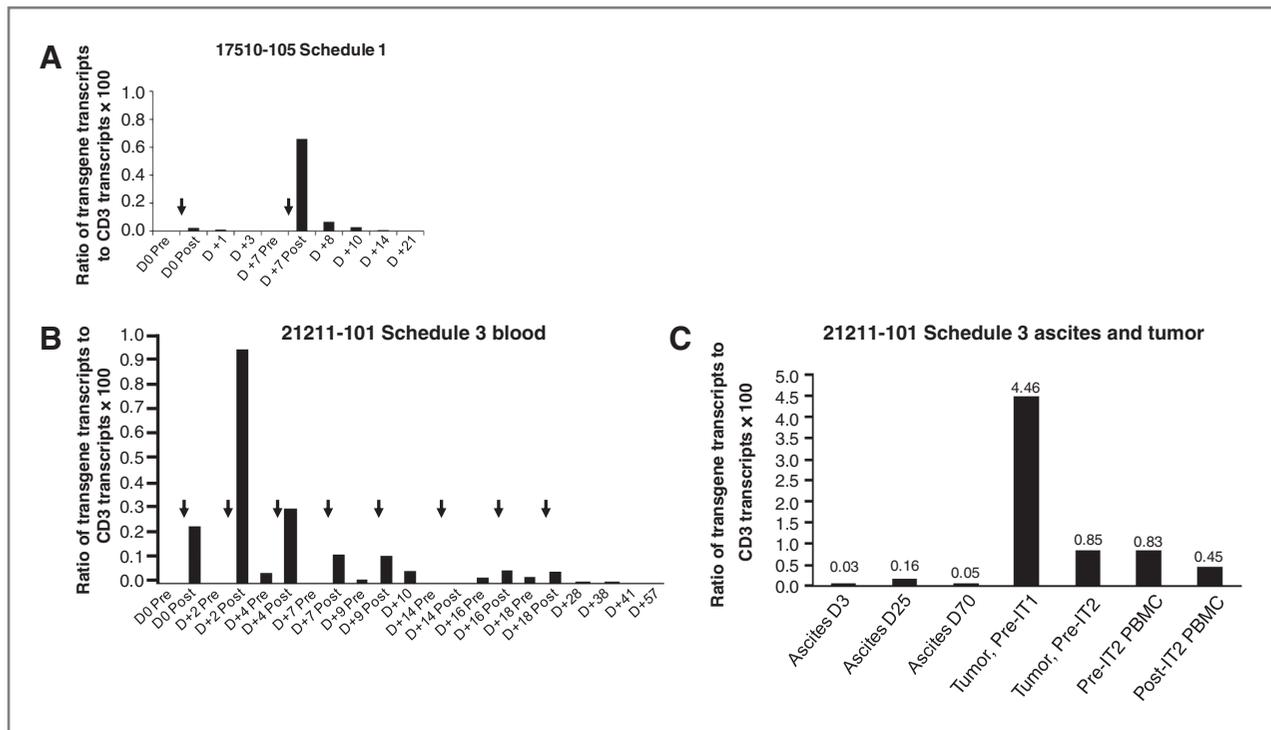
Figure 2. *In vivo* persistence of CARTmeso cells and trafficking to primary and metastatic tumor sites. RNA was isolated from whole blood on the indicated day before (Pre) and after (Post) CARTmeso cell infusion (black arrows). The relative amount of CARTmeso and CD3ε transcripts with normalization to the housekeeping gene *PP1B* was determined. Shown is the ratio of CARTmeso transgene transcripts to CD3ε transcripts × 100 for MPM patient 17510-105 during (A) schedule 1. The arrows indicate injection of 10^8 and 10^9 CARTmeso cells on day 0 and day 7. B, the ratio of CARTmeso transgene transcripts to CD3ε transcripts × 100 within whole blood for PDA patient 21211-101 during schedule 3 is shown. The arrows indicate injection of 3×10^8 CARTmeso cells i.v. C, the ratio of CARTmeso transgene transcripts to CD3ε transcripts × 100 within ascites on days +3 and +25 after i.v. CARTmeso cell infusion, within ascites on day +70 after intratumoral CARTmeso cell injection, within primary pancreatic tumor tissue before intratumoral injection with CARTmeso cells on day +35 (tumor, Pre IT1) and day +57 (tumor, Pre IT2) and within peripheral blood mononuclear cells before (Pre IT2 PBMC) and after (Post IT2 PBMC) intratumoral injection with CARTmeso cells on day +57 is shown. See Supplementary Fig. S1 for details on cell injection dose and schedule.
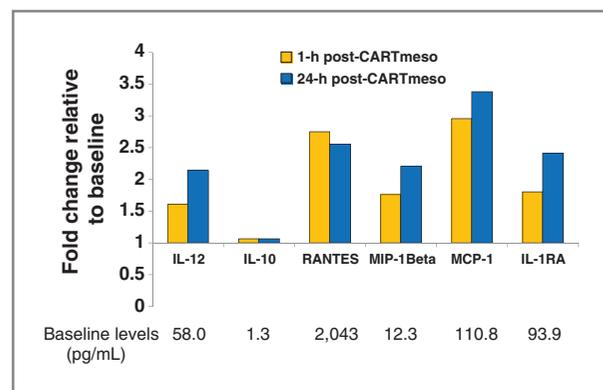
Bioactivity of RNA CARTmeso cells

The impact of CARTmeso cell infusion on immune activation in the patients was examined by soluble immune factor profiling of serum samples collected at defined time points. From this analysis of a panel of 30 cytokines, chemokines, and other soluble factors, variable responses were seen. No significant changes were seen in patient 17510-105 after the first 2 doses; however, a transient cytokine release syndrome occurred after the third infusion with large elevations in IL-6 and chemokines such as MCP-1 (20). The cytokines remained elevated for 4 days in this patient. In contrast, after the first CARTmeso cell infusion in PDA patient 21211-101, modest increases in MIP1β, IL-12, MCP-1, and IL-1Rα were detected within 1 hour (Fig. 3). Changes in the levels of these cytokines persisted throughout the course of treatment with the levels of IL-12 and IL-1Rα returning to near baseline 10 days after the last CARTmeso cell i.v. infusion (Supplementary Fig. S3). Intratumoral injection of CARTmeso cells also produced a modest increase in the levels of IL-12 and IL-1Rα within 3 days of injection. These findings are consistent with the induction of a cellular immune response *in vivo* following infusion of CARTmeso cells.

To confirm the bioactivity of CARTmeso cells, we determined the capacity of CARTmeso cells generated for patient 21211-101 to recognize and lyse human pancreatic tumor cell lines, including a cell line derived from the patient's own ascites fluid (Supplementary Fig. S4). From this analysis, we determined that CARTmeso cells can recognize and lyse pancreatic tumor cell lines that express mesothelin. Specific and potent lysis was also observed for the patient's own tumor cells, suggesting the possibility that the decrease in tumor cells within the patient's ascites may have been a result of direct killing by the infused CARTmeso cells.

Induction of humoral epitope spreading after RNA CARTmeso cell infusion

We hypothesized that CARTmeso cells, if able to recognize and lyse primary tumor cells *in vivo*, might elicit a systemic antitumor immune response. To examine this hypothesis, we conducted high-throughput serologic analyses of antibody responses to antigens to detect the development of a polyclonal immune response that may have occurred as a result of tumor destruction and epitope spreading. These analyses used an unbiased interrogation of treatment-induced IgG responses to almost 10,000 independent human proteins. In PDA patient 21211-101, new antibody responses were detected at day +44 to more than 100 proteins. Responses that were elevated at least 10-fold in postinfusion samples compared with baseline were detected for 18 proteins (Supplementary Table S4). Elevated antibody responses to these proteins had not been observed in a set of 15 additional protoarray samples conducted for other studies. Similarly, we observed elevated antibody responses to a subset of proteins for patient 17510-105 (Supplementary Table S3). For each patient, antibody responses were detected to some proteins at more than one time point post-CARTmeso cell infusion. Overall, these antibody responses observed in both patients are consistent with CAR T-cell–mediated tumor destruction leading to the release of self-proteins that are cross-presented in a classical process of epitope spreading.

We also examined pre- and posttreatment sera from both patients for the induction of antitumor immune responses by immunoblotting using purified tumor-associated proteins or protein lysates from human MPM or PDA cell lines. Antitumor immune responses were defined by the presence of new bands or increases in the intensity of pre-existing bands on immunoblots (Fig. 4). No detectable SV40 T antigen antibodies were seen at baseline or after CARTmeso infusion in the patient with mesothelioma. At baseline, we observed low antibody levels against the 37-kDa purified mesothelin protein (lanes marked Meso in Fig. 4) in patients 17510-105 and 21211-101. After CARTmeso cell administration, no significant change in antimesothelin antibodies was observed. However, for patient 21211-101, a marked increase in antimesothelin antibodies was detected on day +57 of schedule 3 (Fig. 4B, blue arrow). This antibody response was transient and returned to baseline levels by day +92. Further antibody pattern alterations were observed after CARTmeso cell infusion in patients 17510-105 (Fig. 4A) and 21211-101 (Fig. 4B). For example, in the posttreatment sera of patient 17510-105, there was an increase in antibodies detecting a 48-kDa protein and a ∼75-kDa protein present in multiple allogeneic cell lines (Fig. 4A, red boxes). For patient 21211-101, antibodies against multiple proteins present in an allogeneic cell line (Panc-1) and an autologous cell line derived from the patient's own ascites fluid were detected (Fig. 4B, boxes). For instance, several new antibodies were detected in the 64- to 80-kDa regions at day +64 that were less abundant or absent at day +99. In addition, several new antibodies could be detected at day +99 that were not observed at baseline or at day +64. These findings, along with the protoarray analysis, suggest that an antitumor humoral immune response was induced by CARTmeso cell infusion.

Discussion

CAR T-cell immunotherapy has shown antitumor potency in patients with hematologic malignancies in many trials.
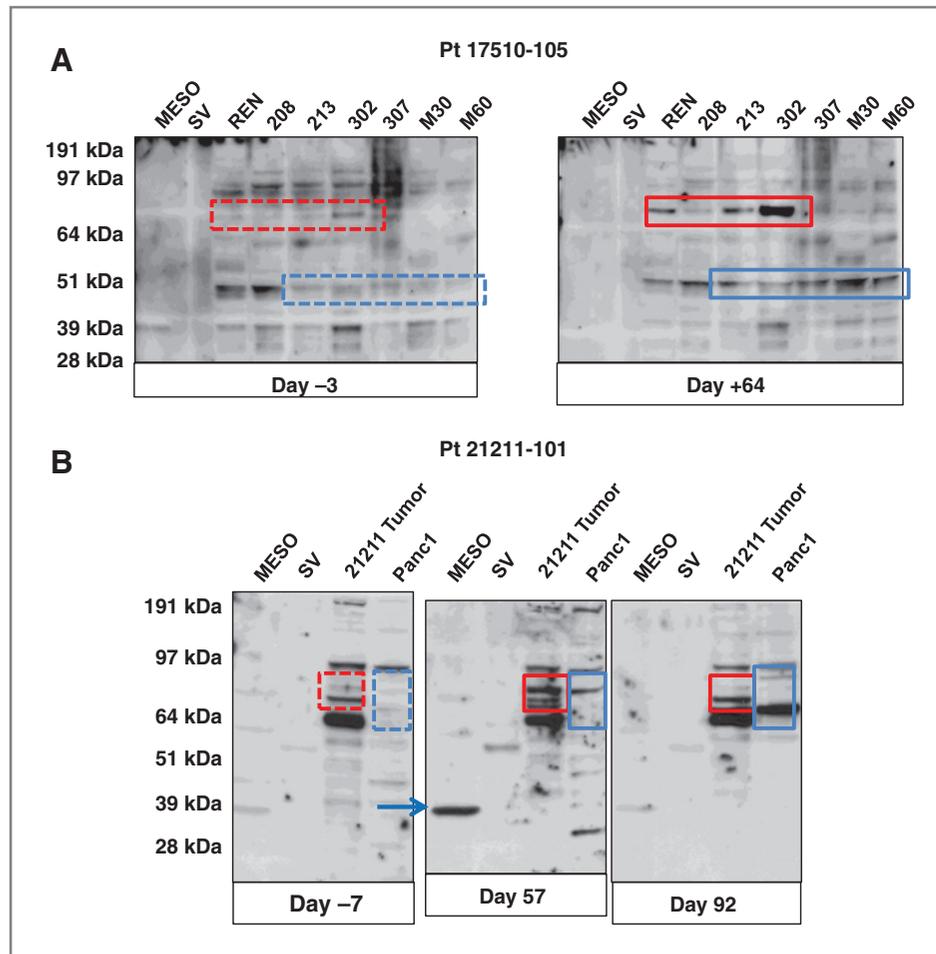

Figure 3. Serum cytokines and chemokines after CARTmeso cell infusion. Fold change in serum cytokines and chemokines in PDA patient 21211-101 on day 0 at 1 and 24 hours after the first i.v. CARTmeso cell infusion. Baseline levels (pg/mL) of cytokines/chemokines are shown below each corresponding soluble factor.

Figure 4. CARTmeso cell induction of antitumor antibodies. Sera obtained from patients pre- and post-CARTmeso therapy was analyzed for the presence of antibodies reactive with mesothelin and with cell extracts from autologous and allogeneic tumor cell lines. A, sera from MPM patient 17510-105 obtained at day −3 and day +64 were analyzed by immunoblotting for reactivity against purified mesothelin protein (MESO), SV40 large T antigen protein (SV), and lysates obtained from seven mesothelioma cell lines (REN, 208, 213, 302, 307, M30, and M60). New bands at ~70 kDa (red boxes) and ~45 kDa (blue boxes) were seen after CARTmeso cell infusion. B, sera from PDA patient 21211-101 obtained at days −7, +57, and +92 were analyzed by immunoblotting for reactivity against mesothelin protein (MESO), SV40 large T antigen protein (SV), lysate from a PDA cell line (Panc1), and lysate from a tumor cell line derived from the patient's own ascites (21211 tumor). A strong antimesothelin band was noted in the day +57 sample (blue arrow), and new bands were seen after receiving CARTmeso cell infusion at ~65 to 80 kDa (red boxes) for the autologous 21211 cell line and for the Panc1 cell lines (blue boxes).

However, with the exception of pediatric neuroblastoma (21), CAR T-cell approaches have not shown antitumor effects in solid malignancies. This is, in part, due to the development of off-tumor on-target toxicities as has been observed in CAR-based clinical studies that have targeted carbonic anhydrase IX (CAIX), which is overexpressed on renal cell carcinoma but which is also expressed at low levels on normal tissues, including the liver (5, 6). For this reason, it is critical to consider potential off-target toxicities and strategies to mitigate these toxicities in the early clinical development of CAR T-cell approaches for solid malignancies. Here, we have shown the feasibility of using mRNA CAR T cells to explore the safety and bioactivity of mesothelin-redirected CAR T cells in patients with advanced MPM and PDA. Our findings show that CARTmeso cells had acceptable safety after delivery by intravenous and intratumoral routes of injection and mediated antitumor activity in vivo, including the induction of epitope spreading. We observed evidence of antitumor activity despite the transient nature of CAR T cells and a lack of pretreatment lymphodepletion. A recent study has shown a promising potential in combining CAR T-cell therapy with checkpoint blockade (22).

We are exploring three treatment schedules designed to evaluate the safety of cell doses, repeated infusions, and route of administration. Both patients treated with CARTmeso cells developed antimurine CARTmeso antibody responses. For the patient with MPM, this antibody response was the cause of an anaphylactic event that occurred upon reinitiating CARTmeso cell infusions after a 4-week treatment interruption (20). On the basis of this finding, we have modified our ongoing clinical trials evaluating RNA CARTmeso cell therapy in MPM (NCT01355965) and PDA (NCT01897415) to prohibit infusion breaks lasting more than 10 days to avoid IgE class switching that can occur during this time interval. Given the reduced levels of CARmeso T-cell persistence with repeated infusions, we believe that the use of humanized or fully human scFv will be required, unlike the case with CD19-directed CARs that induce B-cell aplasia.

Given the CARTmeso cell bioactivity in vivo, we did not observe overt evidence for off-tumor toxicities (e.g., pleuritis, pericarditis, and peritonitis). In previous studies with anti-mesothelin antibody–toxin drug conjugates, pleuritis was a dose-limiting toxicity (23). However, unlike antibody-based therapies targeting mesothelin, which have a biodistribution that is largely dependent on diffusion capacity into tissues, CARTmeso cells must traffic to normal tissues to directly mediate off-tumor toxicities. We hypothesize that in the absence of an inflammatory response to recruit CARTmeso

cells into these normal tissues, CARTmeso targeting of mesothelin-expressing normal tissues may be limited. Formal testing of this hypothesis will require further investigation using frequent and repetitive dosing of CARTmeso cells in more patients.

Our finding that the levels of CARTmeso transcripts were detectable only transiently within the peripheral blood after CARTmeso cell infusion was expected on the basis of preclinical studies (16, 17). We found that the levels of CARTmeso transcripts were measurable following each infusion with levels detected correlating with infusion dose. To address the trafficking of CARTmeso cells to tumor tissues, we detected CARTmeso transcripts in ascites fluid 3 days after the initial CARTmeso cell infusion. Unexpectedly, we also detected CARTmeso transcripts within ascites fluid 7 days after the last i.v. infusion of CARTmeso cells and within a tumor biopsy collected 17 days after the last i.v. infusion of CARTmeso cells. Overall, these findings indicate that CARTmeso cells can traffic to and persist in tumor tissues.

The development of a broad tumor-specific adaptive immune response due to epitope spreading as a consequence of tumor destruction and inflammation has long been proposed to be an important secondary mechanism underlying the potency of immunotherapy. However, without a clearly identified tumor antigen in a vaccine setting, it is difficult to detect specific antitumor lymphocyte responses (24). For this reason, we used immunoblot and protoarray analyses to evaluate the development of humoral immunity following CARTmeso cell infusion. This approach has been used by other investigators to identify antitumor immunity following various immunotherapies (25–27). In our study, both patients with clinical responses to CARTmeso therapy also developed new antitumor responses detectable on Western blot analysis. Antibody responses to a number of self-proteins were also detected by protoarray following CARTmeso cell infusion in both patients. Among the molecules, most robustly recognized by antibodies in the patient with PDA were Septin 6 and density-regulated protein. Septin 6 is a GTPase belonging to the septin family of proteins involved in cytokinesis and by virtue of alternative splicing and overexpression has been implicated in neoplasia (28, 29). Density-regulated protein modulates the expression of cancer-related transcripts and is overexpressed in epithelial (e.g., ovarian and breast) cancers (30). In patient 17510-105, we detected an antibody response recognizing p21 (CDKN1A)-activated kinase (PAK6). PAKs are key regulators of cell motility/migration, survival, proliferation, and gene transcription. PAK hyperactivation has been observed in mesothelioma and other tumor types, including breast cancer, colon cancer, and melanoma (31). However, the majority of antibodies detected by the protoarray analysis

recognized proteins that are not expressed on the surface of cells, overexpressed by cancer, nor implicated in the malignant process. We believe that this response may reflect the breadth and robustness of the humoral immune response induced by CART immunotherapy. Overall, our findings of humoral epitope spreading induced by CARTmeso therapy have significant implications for the role of CAR therapy in stimulating broad antitumor adaptive immunity. The clinical activity, trafficking of CART cells to tumor tissues, and evidence of epitope spreading suggest that mRNA CAR T-cell therapy is a promising treatment modality for patients with solid malignancies.

Disclosure of Potential Conflicts of Interest

Authors' Contributions

Conception and design: G.L. Beatty, A.R. Haas, B. Levine, S.M. Albelda, M. Kalos, C.H. June
Development of methodology: G.L. Beatty, A.R. Haas, B. Levine, M. Kalos
Acquisition of data (provided animals, acquired and managed patients, provided facilities, etc.): G.L. Beatty, A.R. Haas, M. Soulen, B. Levine, S.M. Albelda, M. Kalos
Analysis and interpretation of data (e.g., statistical analysis, biostatistics, computational analysis): G.L. Beatty, A.R. Haas, M.V. Maus, D.A. Torigian, B. Levine, S.M. Albelda, M. Kalos, C.H. June
Writing, review, and/or revision of the manuscript: G.L. Beatty, A.R. Haas, M.V. Maus, D.A. Torigian, M. Soulen, B. Levine, S.M. Albelda, M. Kalos, C.H. June
Administrative, technical, or material support (i.e., reporting or organizing data, constructing databases): G.L. Beatty, M.V. Maus, B. Levine
Study supervision: G.L. Beatty, A.R. Haas, M. Kalos, C.H. June

Acknowledgments

Grant Support

References

1. Kochenderfer JN, Dudley ME, Feldman SA, Wilson WH, Spaner DE, Maric I, et al. B-cell depletion and remissions of malignancy along with cytokine-associated toxicity in a clinical trial of anti-CD19 chimeric-antigen-receptor-transduced T cells. Blood 2012;119:2709–20.

2. Brentjens RJ, Davila ML, Riviere I, Park J, Wang X, Cowell LG, et al. CD19-targeted t cells rapidly induce molecular remissions in adults with chemotherapy-refractory acute lymphoblastic leukemia. Sci Transl Med 2013;5:177ra38.

3. Porter DL, Levine BL, Kalos M, Bagg A, June CH. Chimeric antigen receptor-modified T cells in chronic lymphoid leukemia. N Engl J Med 2011;365:725–33.

4. Grupp SA, Kalos M, Barrett D, Aplenc R, Porter D, Rheingold S, et al. Chimeric antigen receptor-modified T cells for acute lymphoid leukemia. N Engl J Med 2013;368:1509–18.

5. Lamers CH, Sleijfer S, van Steenbergen S, van Elzakker P, van Krimpen B, Groot C, et al. Treatment of metastatic renal cell carcinoma with CAIX CAR-engineered T cells: clinical evaluation and management of on-target toxicity. Mol Ther 2013;14:904–12.

6. Lamers CH, Sleijfer S, Vulto AG, Kruit WH, Kliffen M, Debets R, et al. Treatment of metastatic renal cell carcinoma with autologous T-lymphocytes genetically retargeted against carbonic anhydrase IX: first clinical experience. J Clin Oncol 2006;24:e20–2.

7. Di Stasi A, Tey SK, Dotti G, Fujita Y, Kennedy-Nasser A, Martinez C, et al. Inducible apoptosis as a safety switch for adoptive cell therapy. N Engl J Med 2011;365:1673–83.

8. Kalos M, June CH. Adoptive T cell transfer for cancer immunotherapy in the era of synthetic biology. Immunity 2013;39:49–60.

9. Argani P, Iacobuzio-Donahue C, Ryu B, Rosty C, Goggins M, Wilentz RE, et al. Mesothelin is overexpressed in the vast majority of ductal adenocarcinomas of the pancreas: identification of a new pancreatic cancer marker by serial analysis of gene expression (SAGE). Clin Cancer Res 2001;7:3862–8.

10. Chang K, Pastan I. Molecular cloning of mesothelin, a differentiation antigen present on mesothelium, mesotheliomas, and ovarian cancers. Proc Natl Acad Sci U S A 1996;93:136–40.

11. Ho M, Hassan R, Zhang J, Wang QC, Onda M, Bera T, et al. Humoral immune response to mesothelin in mesothelioma and ovarian cancer patients. Clin Cancer Res 2005;11:3814–20.

12. Thomas AM, Santarsiero LM, Lutz ER, Armstrong TD, Chen YC, Huang LQ, et al. Mesothelin specific CD8+ T cell responses provide evidence of in vivo cross-priming by antigen presenting cells in vaccinated pancreatic cancer patients. J Exp Med 2004;200: 297–306.

13. Kelly RJ, Sharon E, Pastan I, Hassan R. Mesothelin-targeted agents in clinical trials and in preclinical development. Mol Cancer Ther 2012; 11:517–25.

14. Hassan R, Miller AC, Sharon E, Thomas A, Reynolds JC, Ling A, et al. Major cancer regressions in mesothelioma after treatment with an anti-mesothelin immunotoxin and immune suppression. Sci Transl Med 2013;5:208ra147.

15. Carpenito C, Milone MC, Hassan R, Simonet JC, Lakhal M, Suhoski MM, et al. Control of large, established tumor xenografts with genetically retargeted human T cells containing CD28 and CD137 domains. Proc Natl Acad Sci U S A 2009;106: 3360–5.

16. Zhao Y, Moon E, Carpenito C, Paulos CM, Liu X, Brennan A, et al. Multiple injections of electroporated autologous T cells expressing a chimeric antigen receptor mediate regression of human disseminated tumor. Cancer Res 2010;70:9062–72.

17. Barrett DM, Zhao Y, Liu X, Jiang S, Carpenito C, Kalos M, et al. Treatment of advanced leukemia in mice with mRNA engineered T cells. Hum Gene Ther 2011;22:1575–86.

18. Barrett DM, Liu X, Jiang S, June CH, Grupp SA, Zhao Y. Regimen-specific effects of RNA-modified chimeric antigen receptor T cells in mice with advanced leukemia. Hum Gene Ther 2013;24:717–27.

19. Kalos M, Levine BL, Porter DL, Katz S, Grupp SA, Bagg A, et al. T cells expressing chimeric receptors establish memory and potent antitumor effects in patients with advanced leukemia. Sci Transl Med 2011; 3:95ra73.

20. Maus MV, Haas AR, Beatty GL, Albelda SM, Levine BL, Liu X, et al. T cells expressing chimeric antigen receptors can cause anaphylaxis in humans. Cancer Immunol Res. Published Online First April 7, 2013; doi: 10.1158/2326-6066.

21. Louis CU, Savoldo B, Dotti G, Pule M, Yvon E, Myers GD, et al. Antitumor activity and long-term fate of chimeric antigen receptor-positive T cells in patients with neuroblastoma. Blood 2011;118: 6050–6.

22. John LB, Devaud C, Duong CM, Yong C, Beavis PA, Haynes NM, et al. Anti-PD-1 antibody therapy potently enhances the eradication of established tumors by gene-modified T cells. Clin Cancer Res 2013; 19:5636–46.

23. Hassan R, Bullock S, Premkumar A, Kreitman RJ, Kindler H, Willingham MC, et al. Phase I study of SS1P, a recombinant anti-mesothelin immunotoxin given as a bolus I.V. infusion to patients with mesothelin-expressing mesothelioma, ovarian, and pancreatic cancers. Clin Cancer Res 2007;13:5144–9.

24. Disis ML. Immunologic biomarkers as correlates of clinical response to cancer immunotherapy. Cancer Immunol Immunother 2011;60: 433–42.

25. Fonseca C, Soiffer R, Ho V, Vanneman M, Jinushi M, Ritz J, et al. Protein disulfide isomerases are antibody targets during immune-mediated tumor destruction. Blood 2009;113:1681–8.

26. Gnjatic S, Ritter E, Buchler MW, Giese NA, Brors B, Frei C, et al. Seromic profiling of ovarian and pancreatic cancer. Proc Natl Acad Sci U S A 2010;107:5088–93.

27. Marina O, Hainz U, Biernacki MA, Zhang W, Cai A, Duke-Cohan JS, et al. Serologic markers of effective tumor immunity against chronic lymphocytic leukemia include nonmutated B-cell antigens. Cancer Res 2010;70:1344–55.

28. Russell SE, Hall PA. Do septins have a role in cancer? Br J Cancer 2005;93:499–503.

29. Hall PA, Jng K, Hillan KJ, Russell SE. Expression profiling the human septin gene family. J Pathol 2005;206:269–78.

30. Oh JJ, Grosshans DR, Wong SG, Slamon DJ. Identification of differentially expressed genes associated with HER-2/neu overexpression in human breast cancer cells. Nucleic Acids Res 1999;27:4008–17.

31. Menges CW, Sementino E, Talarchek J, Xu J, Chernoff J, Peterson JR, et al. Group I p21-activated kinases (PAKs) promote tumor cell proliferation and survival through the AKT1 and Raf-MAPK pathways. Mol Cancer Res 2012;10:1178–88.

Correction: Mesothelin-Specific Chimeric Antigen Receptor mRNA-Engineered T Cells Induce Antitumor Activity in Solid Malignancies

In this article (Cancer Immunol Res 2014;2:112–20), which appeared in the February 2014 issue of *Cancer Immunology Research* (1), the description of antibody pattern alterations after CARTmeso cell infusion in patient 21211-101 in the Results section on page 117 is incorrect and does not match that shown in Fig. 4B. During the preparation of the original manuscript, the figure listed sampling days of 0, 64, and 99. During the revision process, the authors discovered that the days in Fig. 4B were mislabeled and the samples were actually from Days −7, 57, and 92, as described in the original figure legend. Panel B of the figure was updated and is correct as published. However, the text was not updated and should be corrected to read:

"For instance, several new antibodies were detected in the 64- to 80-kDa regions at day +57 that were less abundant or absent at day +92. In addition, several new antibodies could be detected at day +92 that were not observed at baseline or at day +57."

Also, the Supplementary Data for the article was not updated; the final sentence of the Supplemental Results should read as follows:

"HACA responses became detectable in PDA patient 21211-101 after completing Schedule 3 (day +57) (Fig. S2)."

The final sentence of the Supplementary Fig. S2 legend should read as follows:

"Post-serum time points for each patient are as follows: MPM 17510-105 − day +44; and PDA 21211-101 − day +57."

The Supplementary Data has been updated on the online journal.

Reference

1. Beatty GL, Haas AR, Maus MV, Torigian DA, Soulen MC, Plesa G, et al. Mesothelin-specific chimeric antigen receptor mRNA-engineered T cells induce antitumor activity in solid malignancies. Cancer Immunol Res 2014;2:112–20.

AAGR American Association for Cancer Research

Cancer Immunology Research

Mesothelin-Specific Chimeric Antigen Receptor mRNA-Engineered T Cells Induce Antitumor Activity in Solid Malignancies

Gregory L. Beatty, Andrew R. Haas, Marcela V. Maus, et al.

Updated version	Access the most recent version of this article at: doi:10.1158/2326-6066.CIR-13-0170
Supplementary Material	Access the most recent supplemental material at: http://cancerimmunolres.aacrjournals.org/content/suppl/2015/01/21/2326-6066.CIR-13-0170.DC2

Cited articles	This article cites 30 articles, 19 of which you can access for free at: http://cancerimmunolres.aacrjournals.org/content/2/2/112.full#ref-list-1
Citing articles	This article has been cited by 66 HighWire-hosted articles. Access the articles at: http://cancerimmunolres.aacrjournals.org/content/2/2/112.full#related-urls

E-mail alerts	Sign up to receive free email-alerts related to this article or journal.
Reprints and Subscriptions	To order reprints of this article or to subscribe to the journal, contact the AACR Publications Department at pubs@aacr.org.
Permissions	To request permission to re-use all or part of this article, use this link http://cancerimmunolres.aacrjournals.org/content/2/2/112. Click on "Request Permissions" which will take you to the Copyright Clearance Center's (CCC) Rightslink site.